The Journal of Experimental Biology 216, 1850-1861

doi:10.1242/jeb.070938

RESEARCH ARTICLE

Modelling biomechanical requirements of a rider for different horse-riding techniques at trot

Patricia de Cocq[1,2,*], Mees Muller[1], Hilary M. Clayton[3] and Johan L. van Leeuwen[1]

[1]Experimental Zoology Group, Animal Sciences Group, Wageningen UR, PO Box 338, 6700 AH Wageningen, The Netherlands, [2]Biology, Animal and Environment, University of Applied Sciences HAS Den Bosch, PO Box 90108, 5200 MA 's-Hertogenbosch, The Netherlands and [3]Mary Anne McPhail Equine Performance Center, Department of Large Animal Clinical Sciences, College of Veterinary Medicine, Michigan State University, East Lansing, MI 48824, USA

*Author for correspondence (P.deCocq@hasdb.nl)

SUMMARY

The simplest model possible for bouncing systems consists of a point mass bouncing passively on a mass-less spring without viscous losses. This type of spring–mass model has been used to describe the stance period of symmetric running gaits. In this study, we investigated the interaction between horse and rider at trot using three models of force-driven spring (–damper)–mass systems. The first system consisted of a spring and a mass representing the horse that interact with another spring and mass representing the rider. In the second spring–damper–mass model, dampers, a free-fall and a forcing function for the rider were incorporated. In the third spring–damper–mass model, an active spring system for the leg of the rider was introduced with a variable spring stiffness and resting length in addition to a saddle spring with fixed material properties. The output of the models was compared with experimental data of sitting and rising trot and with the modern riding technique used by jockeys in racing. The models show which combinations of rider mass, spring stiffness and damping coefficient will result in a particular riding technique or other behaviours. Minimization of the peak force of the rider and the work of the horse resulted in an 'extreme' modern jockey technique. The incorporation of an active spring system for the leg of the rider was needed to simulate rising trot. Thus, the models provide insight into the biomechanical requirements a rider has to comply with to respond effectively to the movements of a horse.

Supplementary material available online at http://jeb.biologists.org/cgi/content/full/216/10/1850/DC1

Key words: *Equus caballus*, spring–mass model, sitting trot, rising trot, jockey.

Received 3 February 2012; Accepted 19 January 2013

INTRODUCTION

For every role the horse has served since its domestication, from warfare, agriculture and transport to modern-day use as a sports and leisure animal, load carriage has been an important task of these animals. This load carriage has an energetic cost. Taylor and colleagues observed that the metabolic cost increases in direct proportion with the load that an animal has to carry (Taylor et al., 1980). For example, if a horse's load is 20% of body mass, the rate of energy consumption increases by 20%. However, Pearson and colleagues found that, as the load increased, the energy cost per unit mass of the load decreased (Pearson et al., 1998). They suggested that it is more efficient in terms of energy expenditure to carry loads equivalent to 27–40 kg/100 kg of body mass than to carry loads of less than 20 kg/100 kg body mass.

Marsh and co-workers reviewed studies investigating the metabolic response to trunk or head loading (Marsh et al., 2006). Most studies of trunk loading in humans during walking have found that the ratio of the loaded to unloaded net metabolic rate (metabolic ratio) is greater than the ratio of the total mass (of load and body) to the unloaded mass. The studies that have measured the cost of load carriage in humans during running report lower net metabolic ratios than those of the majority of walking studies, but the net metabolic energy ratios are generally greater than the mass ratios. As with the walking data, the trend across these studies is for metabolic energy ratios to approach 1.0 with relatively light loads, indicating that carrying a low load is more efficient, which is in contrast with the study of Pearson and colleagues (Pearson et al., 1998).

In studies of load carrying by humans, strategies to reduce energy expenditure have been identified. African women seem to carry loads on their heads with remarkable efficiency by using their body as a pendulum during locomotion (Heglund et al., 1995). Nepalese porters are able to carry loads in excess of their own body mass up the mountains but the mechanism that enables them to do so is still unknown (Bastien et al., 2005). Abe and colleagues found effects of both walking speed and load position on the energetics of load carriage (Abe et al., 2004; Abe et al., 2008); an energy-saving phenomenon was observed when the load was carried on the back at slower speeds. Another energy-saving mechanism used by people throughout Asia in everyday life is to carry loads on springy bamboo poles. The energy consumption rate using this technique is comparable with the consumption rate using backpacks suspended by springs. The pole suspension system also has the advantage of minimizing peak shoulder forces and peak vertical reaction force, which could help to prevent injuries (Kram, 1991).

Variations in the load also influence energetic costs; the mechanical properties of a backpack (stiffness and damping coefficient) have been shown to affect the energetics of walking in

the human carrying that backpack (Foissac et al., 2009). At an optimal stiffness of the connection between human and backpack, the peak forces on the person decrease, which leads to lower oxygen consumption. This elastic connection can even be used to generate electricity while walking. The application of this principle extends the possibilities for field scientists, explorers and disaster-relief workers to work in remote areas (Rome et al., 2005).

Horses may be required to carry an inanimate load (dead weight) or an animate load (rider). In the case of a rider, both the rider's skill level and the style of riding may affect the interaction between rider and horse. The motion pattern of a horse–rider combination is more consistent for an experienced rider than for an inexperienced rider (Peham et al., 2001). Lagarde and colleagues found the oscillations of the horse's trunk to be less variable for experienced riders than for novice riders (Lagarde et al., 2005); the experienced rider was able to move in phase with the horse whereas the novice rider was not. Schöllhorn and co-workers (Schöllhorn et al., 2006) observed that the movement of the horse, especially the head, was influenced by the rider and that the motion of a professional rider was better adapted to the movement pattern of the horse.

In horse racing, Pfau and colleagues found that race times decreased after jockeys started to use short stirrups and adopted a position in which they were standing in the stirrups (Pfau et al., 2009). The authors hypothesized that the horses were able to gallop faster because the jockeys uncoupled themselves from the horses, which lowered the vertical peak forces and enabled the horses to go faster. At trot, the rider has a choice of three riding styles to accommodate the bouncing motion of the horse's back: sitting, standing or rising. In sitting trot, the rider remains seated in the saddle. In the standing style, the rider's trunk is elevated above the saddle by standing in the stirrups. The modern jockey position is an extreme example of the standing position, characterized by extremely short stirrups and an almost horizontal inclination of the rider's trunk. This technique is most frequently used during gallop races, but it can also be used at trot. In rising trot, the rider alternately sits in the saddle and rises from the saddle during the two successive diagonal stance phases. Therefore, the rider rises out of the saddle during one-half of each complete stride.

Studies on back movements of the horse, ground reaction forces and saddle forces indicate that rising trot is less demanding for the horse than sitting trot. More specifically, thoracolumbar extension has been related to a vertical load on the back of the horse (Slijper, 1946) and an overall greater extension of the thoracolumbar spine has been observed when the rider performed sitting trot compared with an unloaded situation (de Cocq et al., 2009). At rising trot, thoracolumbar extension is similar to sitting trot in the phase when the rider is seated, but resembles the unloaded situation when the rider rises from the saddle (de Cocq et al., 2009). In rising trot, peak vertical ground reaction force is also lower during the standing phase than in the sitting phase (Roepstorff et al., 2009). As there is a linear relationship between peak ground reaction force and the amplitude of the metacarpophalangeal joint angle (McGuigan and Wilson, 2003), this presumably results in a reduced loading of the internal structures in the limb of the horse. Studies of the loading of the horse's back using saddle force measurements (Peham et al., 2010) or rider kinematics (de Cocq et al., 2010) confirmed that peak force on the horse's back is lower during the standing phase of rising trot. Peham and colleagues found a significant reduction in peak force in standing trot compared with sitting or rising trot (Peham et al., 2009). Compared with rising trot, there was no significant difference in peak loading during the phase when the rider sat in the saddle, but peak force was lower in the phase when the rider rose out of the saddle. We found a significant reduction in vertical peak force in rising trot compared with sitting trot in both the sitting and standing phase (de Cocq et al., 2010).

The biomechanical requirements riders have to comply with to perform these different riding techniques are not clear. The objectives of the present study were therefore (1) to propose a simple characterization of the mechanical requirements of a rider using spring (–damper)–mass models, and (2) to evaluate the effect of the biomechanical properties of the rider on stability, the peak force between horse and rider, and the mechanical work of horse and rider. It was hypothesized that the connection between horse and rider has a relatively low spring stiffness in the riding techniques with the least loading and that these riding techniques are examples of strategies that reduce the energy expenditure of the carrier.

MATERIALS AND METHODS

This study was performed with the approval of the All University Committee for Animal Care and Use and the University Committee on Research Involving Human Subjects at Michigan State University, and with full informed consent of the riders.

Experimental setup

Horse and riders

Measurements were taken using one horse (gelding, age 24 years, mass 667 kg, height 1.63 m) and seven experienced female riders with mean ± s.d. age 34±15 years, height 1.69±0.07 m, mass 61.4±5.0 kg. The riders had competed in dressage at intermediate level or higher. A Passier Grand Gilbert dressage saddle (G. Passier and Sohn GmbH, Langenhagen, Germany) was used during the measurements.

Data collection

Three-dimensional kinematic data were collected using eight Eagle infrared cameras recording at 120 Hz using real-time 5.0.4 software (Motion Analysis Corporation, Santa Rosa, CA, USA). A standard right-handed orthogonal Cartesian coordinate system was used. The positive x-axis was oriented in the line of progression of the horse. The positive z-axis was oriented upward and the positive y-axis was oriented perpendicular to the x- and z-axes. The measurement accuracy was estimated by measuring the length of a 500 mm wand that was moved through the field of view; a residual error of 0.55±0.98 mm was found.

To evaluate the vertical movement of rider and horse, infrared light reflective markers were attached to the skin over obvious anatomical locations (supplementary material Fig. S1). The markers on the rider were placed on the skin overlying the approximate joint centres of the shoulder, elbow, wrist, hip and knee, as well as on the head (chin) and back [spinous processes of the 7th cervical (C7) and 12th thoracic (T12) vertebrae]. Markers were also attached to the shoe of the rider over the joint centre of the ankle and on the toe. The riders wore special clothes to enable placement of the markers directly onto the skin. Larger spherical markers were used on the rider's back to ensure that they were visible for the cameras. On the horse, two spherical markers were attached dorsal to the spinous processes of the 6th thoracic (T6) and the 1st lumbar (L1) vertebrae. For determination of stride time, markers were glued to the dorsal sides of the hind hooves.

Measurements were taken at trot in a straight line on a rubberized surface that was adherent to the underlying concrete floor under two conditions performed in random order: rising trot and sitting trot. Each rider chose whether to rise from the saddle during the right or left diagonal step. The average forward speed of a trial was

calculated by numerical differentiation using the position of the marker on L1 and trials of one horse–rider combination within a speed range of 0.05 m s^{-1} were retained, with a minimum of six trials within this speed range being recorded for each condition. The mean ± s.d. speed of all horse–rider combinations was 3.26±0.10 m s^{-1}. One full stride was extracted from each trial and four full strides were analysed for each horse–rider combination at sitting trot and rising trot.

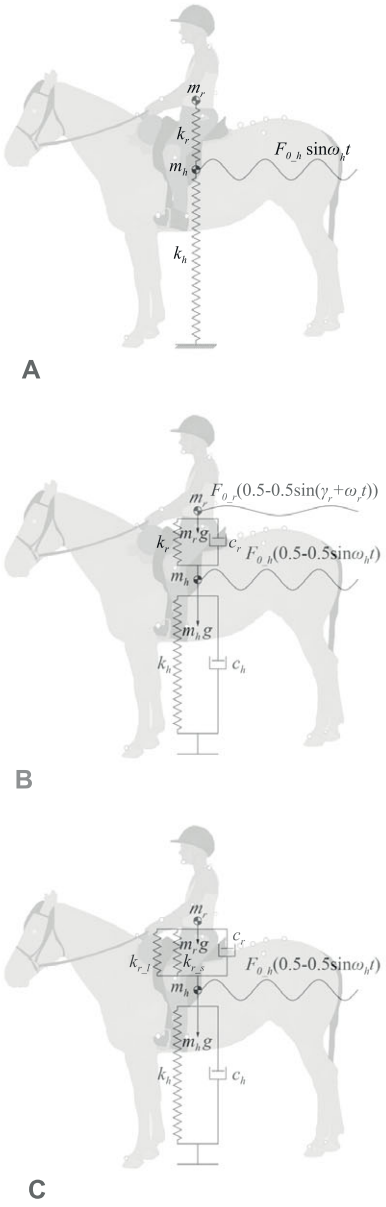

Fig. 1. Mechanical models of horse–rider interaction. (A) Simple spring–mass model. (B) Spring–damper–mass model with forcing function of the rider. (C) Spring–damper–mass model with active spring system of the leg of the rider. m_h, mass of the horse; m_r, mass of the rider; k_h, spring of the horse; k_r, spring of the rider; $k_{r,s}$, saddle spring of the rider; $k_{r,l}$, active spring system of the leg of the rider; c_h, damping coefficient of the horse; c_r, damping coefficient of the rider; $F_{0,h}$, amplitude of the forcing function of the horse; ω_h, angular frequency of the forcing function of the horse; t, time; $F_{0,r}$, amplitude of the forcing function of the rider; γ_r, phase difference of the forcing function of the rider; and ω_r, angular frequency of the forcing function of the rider.

Data processing

Reconstruction of the 3D position of each marker was based on a direct linear transformation algorithm. The raw coordinates were imported into Matlab (The MathWorks Inc., Natick, MA, USA) for further data analysis. Individual stride cycles were determined, with the beginning of each stride cycle defined as the moment of contact of the hind hoof that was grounded when the rider was sitting in the saddle during rising trot. Consequently, all riders sat in the saddle during the first half of the stride cycle and rose from the saddle during the second half of the stride cycle. The same hoof sequence was used to define the stride cycle in sitting trot. Detection of the moment of hoof contact was based on the horizontal velocity profile of the marker on the hoof (Peham et al., 1999).

Vertical displacement of the horse was calculated by averaging the z-coordinates of the T6 and L1 markers on the horse. For calculation of the vertical displacement of the centre of mass of the rider, four body segments were defined; foot, lower leg, upper leg and the upper body including the trunk, arms, hands and head. Data on the segmental masses (percentages of body mass) and positions of segmental mass centres (percentages of segment lengths) in female athletes were used (Zatsiorsky, 2002). Vertical displacement of the rider's centre of mass can be defined by:

$$z_{\mathrm{r}} = \sum_{i=1}^{4} z_{\mathrm{COM},i} m_i / m_{\mathrm{r}} , \quad (1)$$

where subscript r indicates the rider, z is the vertical displacement of the centre of mass, m_i is the mass of the ith segment, $z_{\mathrm{COM},i}$ is the vertical displacement of the centre of mass (COM) of the ith segment and m is the mass. As an equilibrium position is used for the spring–mass model, the average height of horse or rider was subtracted from marker heights at all time points. The vertical displacement time histories were normalized to a 100% stride cycle. Average displacements of the trials were calculated per rider and for the entire group. Standard deviations were calculated from the average displacement patterns of the seven riders. Vertical displacements of horse and rider were plotted against time and against one another.

The simple spring–mass model

The seemingly artificial situation of hopping in place, i.e. at zero forward speed, can be taken as a model for bouncing gaits in animals (Farley et al., 1985). Assuming a linear spring, the following equation of motion during ground contact can be formulated:

$$\sum \mathbf{F}_{\mathrm{h}} = -m_{\mathrm{h}} g - k_{\mathrm{h}}(\delta_{\mathrm{st}} + z_{\mathrm{h}}) = m_{\mathrm{h}} \ddot{z}_{\mathrm{h}} , \quad (2)$$

where subscript h indicates the horse, $\sum\mathbf{F}$ is the sum of the vertical forces, g is the magnitude of the gravitational acceleration, k is the stiffness of the spring, δ_{st} is the static deflection due to the weight of the mass acting on the spring and $\ddot{z}$ is the vertical acceleration. If the static equilibrium position is chosen as a reference for z_{h} (i.e. z_{h}=0), the weight factor can be eliminated and the equation of motion becomes:

$$\sum \mathbf{F}_{\mathrm{h}} = -k_{\mathrm{h}} z_{\mathrm{h}} = m_{\mathrm{h}} \ddot{z}_{\mathrm{h}} . \quad (3)$$

During motion, the horse's body moves up and down rhythmically. As the standing horse does not oscillate in a vertical direction with the force of gravity as the energy source, it is apparent that vertical oscillations have to be excited by a motor system. In the model, the vertical oscillations are caused by a forcing function which is described as a sine wave function (Rooney, 1986). The equation of motion therefore becomes:

$$\sum \mathbf{F}_{\mathrm{h}} = m_{\mathrm{h}} \ddot{z}_{\mathrm{h}} = -k_{\mathrm{h}} z_{\mathrm{h}} + F_{0,\mathrm{h}} \sin\omega_{\mathrm{h}} t , \quad (4)$$

Table 1. Input parameters of spring–damper–mass models

Input parameter model	Input value	Literature
Mass, rider, simple model (kg)	30–150	Range of rider masses evaluated
Mass, rider, extended models (kg)	60	Average rider
Mass, horse (kg)	600	Average warmblood horse
Spring constant, rider (kN m^{-1})	0–80	Range of rider spring constants evaluated Running: 11–19 kN m^{-1} (Blum et al., 2009) Hopping (60 kg rider): 9–45 kN m^{-1} (Bobbert and Casius, 2011; Farley et al., 1991)
Spring constant, horse (kN m^{-1})	52	Overall leg stiffness calculated according to Farley et al., 1993
Amplitude of forcing function, horse, simple model (N)	3900 (0.1–6000)*	
Amplitude of forcing function, horse, extended models (N)	9900	Gravity added
Frequency of forcing function, horse (Hz)	2.4	Step frequency, horse at trot : 2.4 Hz (this study)
Damping coefficient, rider (kg s^{-1})	0–3000	Range of rider damping coefficients evaluated Leg, human: 300–1900 kg s^{-1} (Zadpoor and Nikooyan, 2010)
Damping coefficient, horse	5000 (0–10000)**	
Rest length, rider (m)	0.60	
Rest length, saddle spring, rider (m)	0.60	
Rest length, leg spring, rider (m)	0.60±0.03	
Rest length, horse (m)	1.24	
Amplitude of forcing function, rider (N)	0–1200	
Frequency, rider (Hz)	1.2	Frequency standing phase, rider
Phase difference, rider	0–2π	

*This range of input values was tested using a contour map of the amplitude and the frequency of the forcing function. The combination of the (known) frequency of 2.4 Hz and an amplitude of 3900 N resulted in a vertical displacement of the horse that was comparable with the experimental data (supplementary material Fig. S2).

**This range of input values was tested using the Downhill Simplex method. This damping coefficient resulted in the best match with the experimental data of horse and rider.

where F_0 is the amplitude of the forcing function, ω is the angular frequency ($2\pi f$, where f is the bouncing frequency) of the forcing function and t is time. The rider–horse interaction can be simulated by adding a second one-dimensional spring–mass system for the rider. Again, we assumed a linear spring and contact between rider and horse. The coupled differential equations for this combined system are (Fig. 1A):

$$\sum \mathbf{F}_\mathrm{h} = m_\mathrm{h}\ddot{z}_\mathrm{h} = -k_\mathrm{h}z_\mathrm{h} - k_\mathrm{r}(z_\mathrm{h} - z_\mathrm{r}) + F_{0,\mathrm{h}}\sin\omega_\mathrm{h} t \,, \quad (5)$$

$$\sum \mathbf{F}_\mathrm{r} = m_\mathrm{r}\ddot{z}_\mathrm{r} = -k_\mathrm{r}(z_\mathrm{r} - z_\mathrm{h}) \,. \quad (6)$$

These coupled differential equations can be solved analytically, resulting in the following:

$$z_\mathrm{h} = -\frac{F_{0,\mathrm{h}}\,(k_\mathrm{r} - m_\mathrm{r}\omega_\mathrm{h}^2)}{m_\mathrm{h}m_\mathrm{r}\omega_\mathrm{h}^4 - (m_\mathrm{h}k_\mathrm{r} + m_\mathrm{r}k_\mathrm{r} + m_\mathrm{r}k_\mathrm{h})\omega_\mathrm{h}^2 + k_\mathrm{h}k_\mathrm{r}}\sin\omega_\mathrm{h} t \,, \quad (7)$$

$$z_\mathrm{r} = -\frac{F_{0,\mathrm{h}}k_\mathrm{r}}{m_\mathrm{h}m_\mathrm{r}\omega_\mathrm{h}^4 - (m_\mathrm{h}k_\mathrm{r} + m_\mathrm{r}k_\mathrm{r} + m_\mathrm{r}k_\mathrm{h})\omega_\mathrm{h}^2 + k_\mathrm{h}k_\mathrm{r}}\sin\omega_\mathrm{h} t \,. \quad (8)$$

During cyclic behaviour, the masses of horse and rider can move either in phase or 180 deg out of phase; other phase relationships are not possible.

The input parameters of the simple spring–mass model are the mass of the rider, the spring constant of the rider, the mass of the horse, the spring constant of the horse, the amplitude of the forcing function of the horse and the frequency of the forcing function of the horse (Table 1). The output parameters are the vertical displacement of the rider and the horse and the vertical forces on the rider and the horse. This basic model was used to evaluate the effect of differences in rider mass and rider spring stiffness on the vertical displacement and force of both horse and rider. The mass of the horse and the frequency of the forcing function were based on the current study. The spring constant of the horse was based on the study of Farley and colleagues (Farley et al., 1993). The amplitude of the forcing function was determined using a contour plot of the frequency of the forcing function and the amplitude of the forcing function and the resulting vertical displacement of the horse (supplementary material Fig. S2).

The spring–damper–mass model with forcing function of the rider

The second spring–damper–mass model incorporated a free-fall for both horse and rider, dampers for both horse and rider and a forcing function for the rider (Fig. 1B). A numerical approach was used, simulating 50 stride cycles with time steps of 0.005 s. As the equations of the model are quite stiff, an appropriate ODE solver (ode15s of Matlab) was used. The extended spring–damper–mass model can be described by the following equations:

$$\sum \mathbf{F}_\mathrm{h} = m_\mathrm{h}\ddot{z}_\mathrm{h} = -\eta_\mathrm{h}c_\mathrm{h}\dot{z}_\mathrm{h} - \eta_\mathrm{r}c_\mathrm{r}(\dot{z}_\mathrm{h} - \dot{z}_\mathrm{r}) - \eta_\mathrm{h}k_\mathrm{h}\varepsilon_\mathrm{h} + \eta_\mathrm{r}k_\mathrm{r}\varepsilon_\mathrm{r} - m_\mathrm{h}g + \eta_\mathrm{h}F_{0,\mathrm{h}}(0.5 - 0.5\sin\omega_\mathrm{h}t) \,, \quad (9)$$

$$\sum \mathbf{F}_\mathrm{r} = m_\mathrm{r}\ddot{z}_\mathrm{r} = -\eta_\mathrm{r}c_\mathrm{r}(\dot{z}_\mathrm{r} - \dot{z}_\mathrm{h}) - \eta_\mathrm{r}k_\mathrm{r}\varepsilon_\mathrm{r} - m_\mathrm{r}g + \eta_\mathrm{r}F_{0,\mathrm{r}}\left(0.5 - 0.5\sin(\gamma_\mathrm{r} + \omega_\mathrm{r}t)\right) \,, \quad (10)$$

$$\varepsilon_\mathrm{h} = (z_\mathrm{h} - z_{\mathrm{h},\eta}) / z_{\mathrm{h},\eta} \,, \quad (11)$$

$$\varepsilon_\mathrm{r} = \left((z_\mathrm{r} - z_\mathrm{h}) - z_{\mathrm{r},\eta}\right) / z_{\mathrm{r},\eta} \,, \quad (12)$$

$$\eta_\mathrm{h} = 0.5 + 0.5\tanh - 10^4\,\varepsilon_\mathrm{h} \,, \quad (13)$$

$$\eta_\mathrm{r} = 0.5 + 0.5\tanh - 10^4\,\varepsilon_\mathrm{r} \,, \quad (14)$$

$$P_\mathrm{h} = \mathbf{F}_\mathrm{h}\dot{z}_\mathrm{h} \,, \quad (15)$$

$$P_\mathrm{r} = \mathbf{F}_\mathrm{r}\dot{z}_\mathrm{r} \,, \quad (16)$$

$$W_\mathrm{h} = \int P_\mathrm{h}\mathrm{d}t \,, \quad (17)$$

$$W_\mathrm{r} = \int P_\mathrm{r}\mathrm{d}t \,, \quad (18)$$

where η_h is the force contact factor of the horse (varying from 0 in suspension phase to 1 in contact phase), η_r is the force contact factor of the rider and $\dot{z}$ is the vertical velocity. These factors were introduced to be able to work with the same differential equations for the contact and suspension phases of rider and horse and to guarantee smooth transitions between the phases. Furthermore, ε is the strain of the leg of the horse or rider, $z_{h,\eta}$, is the height of the horse at the moment just before the suspension phase and $z_{r,\eta}$ is the height of the rider minus the height of the horse just before the rider loses contact with the horse. We have introduced a damping coefficient (c) for the horse and for the rider and a forcing function for the rider.

This model was used to calculate vertical displacement, force, power and work of both horse and rider. The total power of the horse (P_h) and rider (P_r) was calculated using Eqns 15 and 16. Total work of the horse (W_h) and rider (W_r) was calculated using Eqns 17 and 18. The total power and work were calculated using the total forces on horse and rider. A similar approach was followed for the components of these forces (i.e. force of damper, spring and forcing function).

The spring–damper–mass model with active spring system of the leg of the rider

During the sitting phase of the rising trot, the biomechanical properties of the rider are determined by the upper body, the legs and the saddle. During the standing phase, there is no contact between upper body and saddle. This phase will therefore be determined solely by the leg of the rider. When the rider is standing up, muscle activation and changes of geometry will change both the effective stiffness of the leg and the effective rest length of the leg. Therefore, an active spring system for the leg was introduced in the third spring–damper–mass model, instead of the forcing function of the rider (Fig. 1C). The rider was modelled with two springs: a saddle spring (subscript s) with a fixed stiffness and rest length, and a leg spring (subscript l) with a varying stiffness and rest length. The third spring–damper–mass model can be described by the following equations:

$$\begin{aligned} m_h\ddot{z}_h = &-\eta_h c_h \dot{z}_h - \eta_{r,c} c_r (\dot{z}_h - \dot{z}_r) - \eta_h k_h \varepsilon_h \\ &+ \eta_{r,s} k_{r,s} \varepsilon_{r,s} + \eta_{r,s} k_{r,l} \varepsilon_{r,l} - m_h g \\ &+ \eta_h F_{0,h} (0.5 - 0.5 \sin \omega_h t) , \end{aligned} \quad (19)$$

$$m_r\ddot{z}_r = -\eta_{r,c} c_r (\dot{z}_r - \dot{z}_h) - \eta_{r,s} k_{r,s} \varepsilon_{r,s} - \eta_{r,s} k_{r,l} \varepsilon_{r,l} - m_r g , \quad (20)$$

$$k_{r,l} = k_{r,l,base} + k_{r,l,amp} \left(0.5 - 0.5 \sin(\gamma_r + \omega_r t)\right) , \quad (21)$$

$$z_{r,\eta l} = z_{r,\eta l,base} - z_{r,\eta l,amp} \sin(\gamma_r + \omega_r t) , \quad (22)$$

$$\varepsilon_h = (z_h - z_{h,\eta}) / z_{h,\eta} , \quad (23)$$

$$\varepsilon_{r,s} = \left((z_r - z_h) - z_{r,\eta s}\right) / z_{r,\eta s} , \quad (24)$$

$$\varepsilon_{r,l} = \left((z_r - z_h) - z_{r,\eta l}\right) / z_{r,\eta l} , \quad (25)$$

$$\eta_h = 0.5 + 0.5 \tanh -10^4 \varepsilon_h , \quad (26)$$

$$\eta_{r,s} = 0.5 + 0.5 \tanh -10^4 \varepsilon_{r,s} , \quad (27)$$

$$\eta_{r,l} = 0.5 + 0.5 \tanh -10^4 \varepsilon_{r,l} , \quad (28)$$

$$\eta_{r,c} = \eta_{r,s} \text{ if } \eta_{r,s} \geq \eta_{r,l} ; \quad \eta_{r,c} = \eta_{r,l} \text{ if } \eta_{r,s} < \eta_{r,l} , \quad (29)$$

where $k_{r,l}$ is the spring stiffness of the sine wave spring system of the leg of the rider with the base value $k_{r,l,base}$ and an increase of $k_{r,l,amp}$. Furthermore, $z_{r,\eta l}$ is the length of the active spring system of leg of the rider just before the rider loses contact with the horse (rest length), with the base value $z_{r,\eta l,base}$ and the amplitude $z_{r,\eta l,amp}$. This model was used to calculate vertical displacement, force, power and work of both horse and rider during rising trot. Total force, total power and total work of horse and rider were calculated. Furthermore, the components of force, power and work were calculated (i.e. of dampers, springs and forcing function).

Parameter estimation for spring–damper–mass models

The input parameters of the spring–damper–mass models are presented in Table 1. The range of input values was based on values found in the literature (Blum et al., 2009; Bobbert and Casius, 2011; Farley et al., 1991; Farley et al., 1993; Zadpoor and Nikooyan, 2010) or the current study. The Downhill Simplex method (Nelder and Mead, 1965) was used to optimize with regard to vertical displacement of horse and rider, peak force between horse and rider and work of horse and rider. The Downhill Simplex method is a technique for minimizing an objective function in a multi-dimensional space. The method uses the concept of a simplex, with a special polytope of N+1 vertices in N dimensions. The algorithm extrapolates the behaviour of the object function measured at each test point arranged as a simplex and chooses to replace one of the test points with the new test point and so the technique progresses. For the optimization of vertical displacements, the sum of the squared differences between the measured vertical displacement and calculated vertical displacement of both horse and rider were calculated. Phase plots of the last two stride cycles were used to give a graphical overview of the parameter space.

RESULTS

Measured vertical displacement of rider and horse

The experimentally measured vertical displacements (Fig. 2A,B) show a sine wave pattern for the horse and rider during sitting trot, with the rider moving almost in phase with the horse. The movement of the rider is slightly delayed compared with the motion of the horse. During rising trot, however, the pattern of the rider seems to consist of (half) a cosine wave with a long period and a large amplitude (sitting phase) and a cosine wave with a short period and a small amplitude (standing phase). In the figure, the rider may seem to move further downward than the horse, but this is merely the effect of plotting the movements around the mean position of either horse or rider. In fact, the rider is moving more upward than the horse. Phase plots of the measured vertical displacements over a full stride cycle (based on a mean of 28 cycles; seven horse–rider combinations with each four cycles) are shown in Fig. 2C,D. For the sitting trot, we see two very similar loops, which is expected because the vertical motions of the first and the second half of the stride should be rather similar in this riding style. The enclosed surface of the loops is due to the phase difference in the motion of rider and horse. A more complex looping is seen for the rising trot (Fig. 2D). This is mainly caused by the very different motion of the rider in the second part of the stride (compared with the sitting phase). Comparatively, the motion of the horse varies much less than that of the rider, as would be expected given its higher mass and leg forces.

Simulating sitting trot and jockey technique with a simple spring–mass model

With the basic model it is possible to simulate a sitting trot (Fig. 3A). With a relatively high stiffness of the spring, the rider moves in phase with the horse with an amplitude comparable to the experimental data.

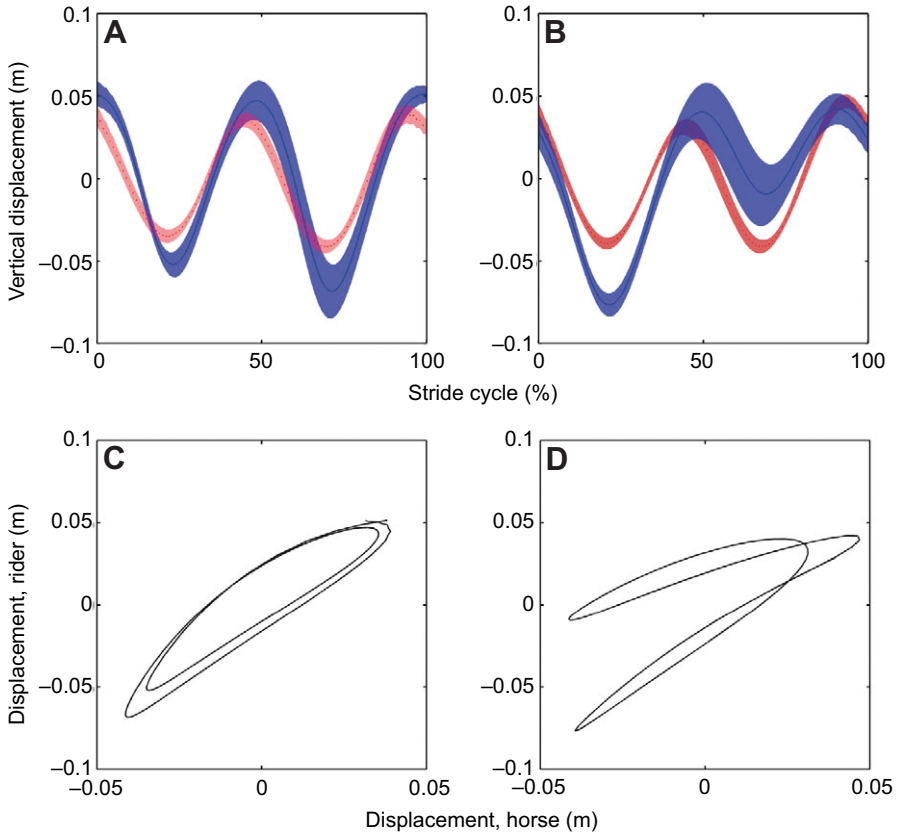

Fig. 2. Vertical displacement of horse and rider during sitting and rising trot. (A) Vertical displacement during sitting trot. (B) Vertical displacement during rising trot. (C) Phase plot of vertical displacement of horse and rider at sitting trot. (D) Phase plot of vertical displacement of horse and rider at rising trot. Red dotted line, displacement of the horse relative to the static equilibrium position of the horse (±s.d., shaded area); blue solid line, displacement of the rider relative to the static equilibrium position of the rider (±s.d., shaded area). Time zero represents contact of the hindlimb, on which the rider sits in the saddle at rising trot. Movements of the horse and rider are plotted around the mean positions of horse and rider, respectively.

The motions of rider and horse are in phase owing to the absence of damping in the model. The movement in counter-phase resembles the movement of a rider adopting jockey technique as described previously (Pfau et al., 2009). The jockey technique can be simulated by the model by using a relatively low stiffness for the rider spring (Fig. 3B). The vertical displacement of the horse is larger and the vertical displacement of the rider is much smaller during the jockey technique. The motions of rider and horse are exactly out of phase because of the absence of damping. The effects of combinations of rider mass and spring stiffness on rider displacement are shown in Fig. 4A. Specific combinations of rider mass and rider stiffness will lead to a vertical displacement of the rider that is in phase with the horse. These combinations can be found in the right half of Fig. 4A and represent sitting trot. Other combinations of rider mass and rider stiffness will lead to a vertical rider displacement that is in counter-phase with the horse. These combinations can be found in the left half of Fig. 4A and represent the jockey technique. Fig. 4B shows the computed displacement for a rider of 60 kg (see horizontal line in Fig. 4A) as a function of spring stiffness of the rider. The jockey technique and sitting trot are again shown on, respectively, the left- and right-hand side of the plot. Between these techniques very large amplitudes occur for a spring stiffness of about 12.5 kN m^{-1}. Fig. 4C and 4D show similar graphs to those in Fig. 4A and 4B, but here the peak forces that occur between horse and rider are plotted. This shows that the jockey technique allows lower peak forces to be used than during sitting trot.

Simulating sitting trot, rising trot and jockey technique with the extended spring–damper–mass models

In the extended spring–damper–mass models, a free-fall was introduced. This free-fall changes the requirements for the stability of the horse–rider system. It is no longer possible that the springs of the model are loaded under tension. Damping is needed to provide stability. Fig. 5 gives an overview of the effects of the spring stiffness and damping coefficient of the rider. The figure indicates where the movements of horse and rider are no longer cyclic (dark grey panels), where the movements are cyclic but the rider temporarily loses contact with the horse (light grey panels), and where the movements are cyclic and the rider remains in contact with the horse (white panels). Combinations of a low damping coefficient and low spring stiffness will result in a phase relationship that resembles the modern jockey technique (i.e. the panel with 5 kN m^{-1} for spring stiffness and 200 kg s^{-1} for damping, Fig. 5). An increase in damping coefficient will result in the sitting trot (second column of panels in Fig. 5). When the spring stiffness is also increased, a lower damping coefficient is needed for a sitting trot (e.g. compare column four with column two in Fig. 5). A very low spring stiffness of the rider (first column of Fig. 5) or low damping (see the dark grey panels on the lower right side of Fig. 5) leads to an unstable non-cyclic behaviour. A high spring stiffness of the rider should be accompanied by relatively high damping to avoid instabilities or undesired large motion amplitudes of the rider (Fig. 5, column five).

The Downhill Simplex method was used to optimize for the measured vertical displacements of horse and rider in sitting and rising trot, peak force of the rider and work of the horse. The combination of spring stiffness and damping coefficient of the rider that resembles the experimentally measured displacements of sitting trot most closely is 23.6 kN m^{-1} and 1056 kg s^{-1} (Fig. 6A,E,I,M,Q). The simulated displacements of horse and rider are very similar to the measured displacements (compare Fig. 6A,E with Fig. 2A,C). Fig. 6I shows that the enclosed loop areas of total force on the rider against its vertical displacement over the stride (number 49 after the start of the simulation) and similarly that for the horse are close to zero. This shows that a very small deviation still occurs from a purely cyclic

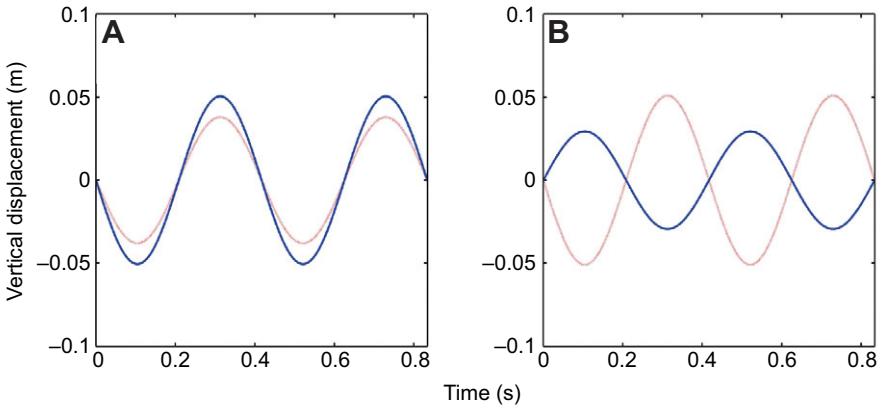

Fig. 3. Displacement of both horse and rider calculated with a basic spring–mass model. (A) Simulation of sitting trot (high rider spring stiffness, 55 kN m^{-1}). (B) Out of phase movement of horse and rider, comparable to vertical movements of horse and rider, with the rider in the jockey position (Pfau et al., 2009) (low rider spring stiffness, 5 kN m^{-1}). Red dotted line, displacement of the horse relative to the static equilibrium position of the horse; blue solid line, displacement of the rider relative to the static equilibrium position of the rider.

behaviour at stride number 49, which is due to the transient effect caused by the deviations of the initial conditions from the cyclical behaviour. The positive and negative work done over the cycle by the forcing functions of rider and horse and their damping should cancel one another out over the stride for cyclic behaviour. Fig. 6M shows power plots for the forcing function, spring and damper of the rider over one stride, as well as the total power of these components. The spring power shows a series of negative and positive phases that correspond to lengthening and shortening of the spring. In between, power is zero, which indicates a free-fall phase with a resting length of the rider's spring. The damping power shows two negative periods with two peaks each and two periods of zero power during the free-fall phase. The power of the forcing function of the rider plays only a very minor role and remains very close to zero. Thus, the forcing function does not compensate for the power losses due to damping of the rider. As the process is cyclic, the net power over the cycle should be zero. The only way to achieve this is by a partial transfer of the power produced by the forcing function of the horse to the rider. Fig. 6Q indeed shows that positive power dominates the fluctuations of the power of the forcing function of the horse. Thus, considerable work is done by this forcing function over the stride. The total work of the horse is 27 J per stride cycle in this riding style. The free-fall phase of the horse is relatively short for the simulated sitting trot and the vertical motion of the horse is relatively limited (compared with the jockey technique, Fig. 6B,F,J,N,R), which is caused by the near in-phase motion of rider and horse.

In the modern jockey technique, the rider has an average displacement of 0.06 m and the rider moves in counter-phase with the horse (Pfau et al., 2009). The combination of spring stiffness and damping coefficient of the rider that resembles this situation the most is 3.3 kN m^{-1} and 10 kg s^{-1} (Fig. 6B,F,J,N,R). The simulated vertical motion of the horse is larger and the vertical

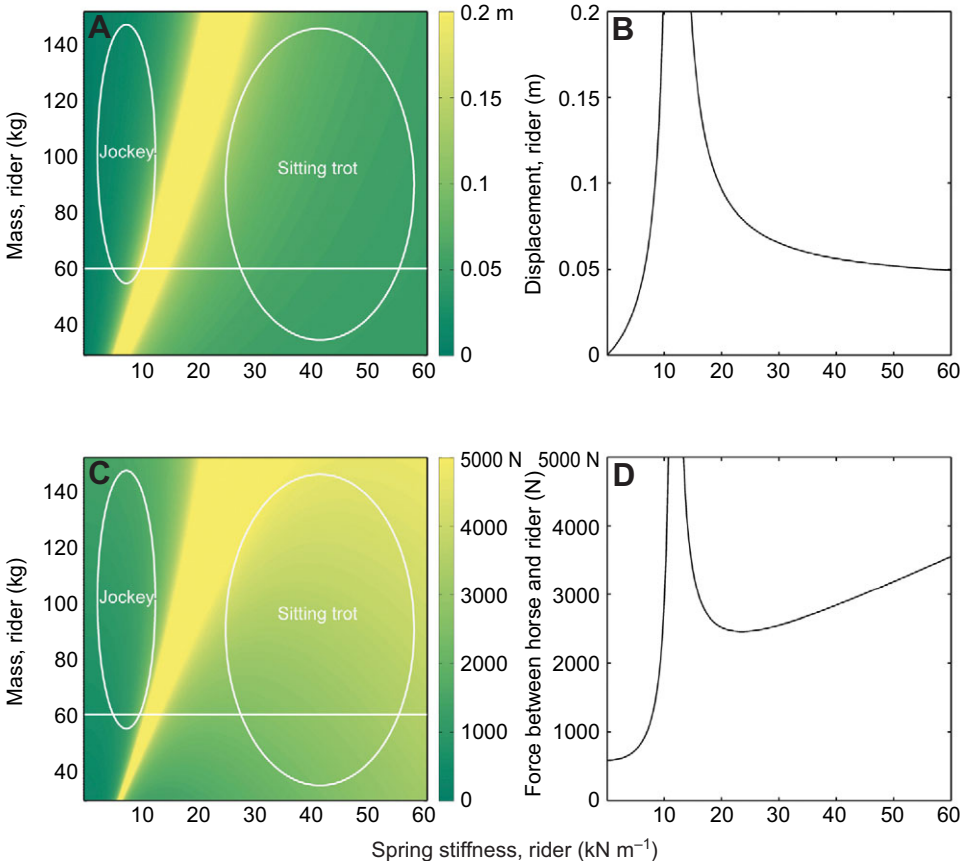

Fig. 4. Effect of combinations of rider mass and rider spring stiffness on vertical displacement and force of the rider. (A) Effect of combinations of rider mass and rider spring stiffness on vertical displacement of the rider (m). (B) Effect of spring stiffness on vertical displacement of a 60 kg rider (peak value, 10.60 m). (C) Effect of combinations of rider mass and rider spring stiffness on force between the horse and rider (N). (D) Effect of spring stiffness on force between the horse and a 60 kg rider (peak value, 1.25×10^5 N). A and C illustrate the effects of rider mass and rider spring stiffness on the rider's displacement (A) and on the force between horse and rider (C). The graphs illustrate the fact that low spring stiffness is associated with the standing (jockey) position and high spring stiffness is associated with the sitting position. The ellipses indicate the mass–stiffness combinations that are associated with each rider position. Within each ellipse, for a given spring stiffness, both rider displacement and the force between horse and rider increase with rider mass. B and D use, as an example, a rider of mass 60 kg to show how an increase in spring stiffness affects displacement of the rider (B) and the force between horse and rider (D). Between these two regions of spring stiffness there is a resonance zone with very high and unrealistic displacements and forces.

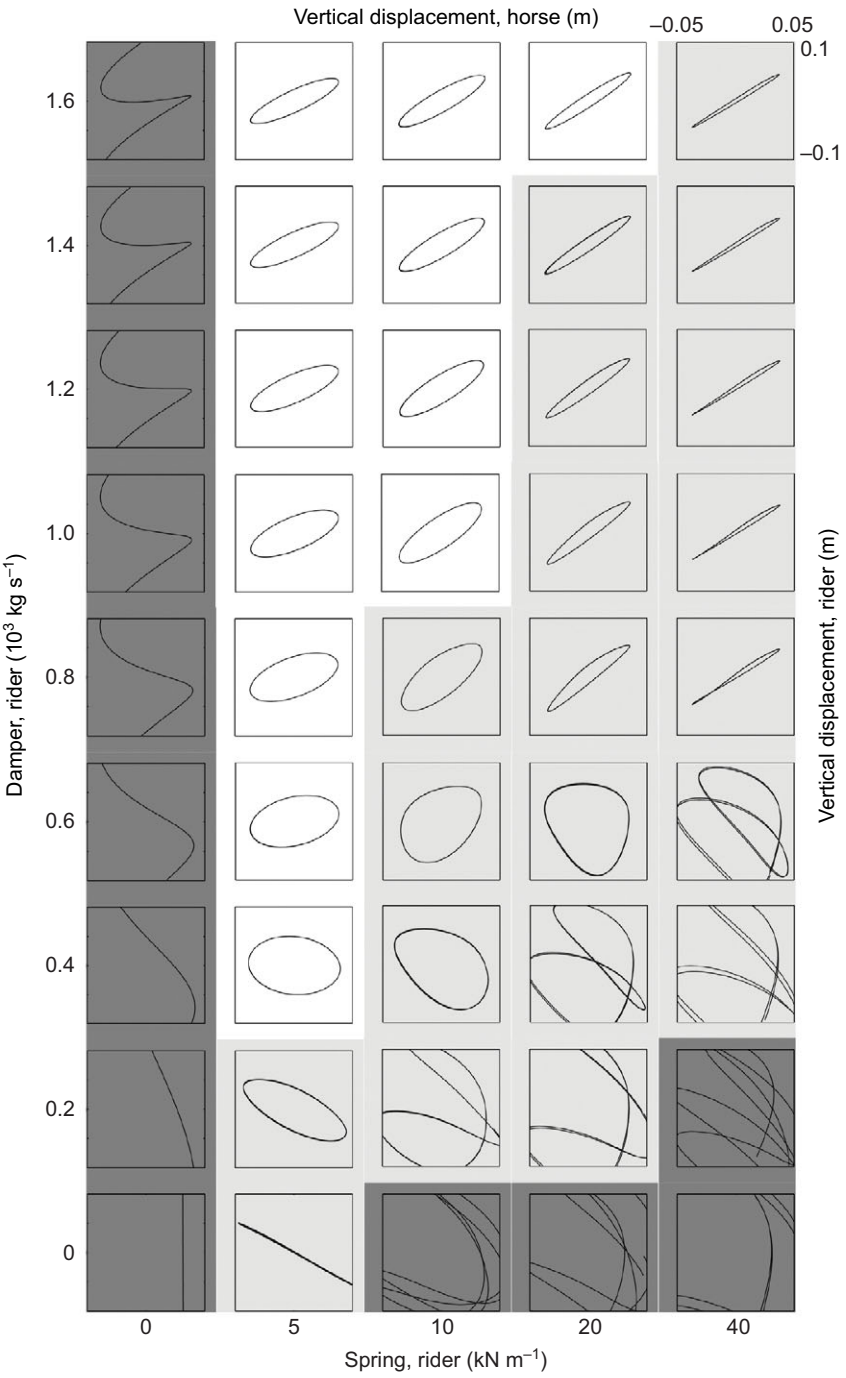

Fig. 5. Phase plots of the displacement of the horse *versus* the displacement of the rider for different values of spring stiffness and damper coefficient of the rider. A combination of a low rider spring stiffness and a low rider damper coefficient results in a phase relationship that resembles the jockey position, whereas a combination of a high rider spring stiffness and a high rider damper coefficient results in a phase relationship that resembles the sitting position. Some combinations lead to phase relationships that do not seem to occur in regular horse riding by experienced persons. This might result in a fall of the rider from the horse. White, cyclic behaviour, with the rider maintaining contact with the horse; dark grey, no cyclic behaviour; light grey, cyclic behaviour, but rider loses contact with horse.

motion of the rider is smaller than the values of sitting trot (compare Fig. 6B and 6A), while the forcing function of the horse is kept the same. The very narrow loop of Fig. 6F indicates that the motion of rider and horse are almost exactly out of phase. The force displacement plots of rider and horse again show loop surfaces that are very close to zero, a result of near-cyclic behaviour. Fig. 6N shows that the power of the forcing function of the rider is again very close to zero and energy losses due to damping are minor compared with those of the simulated sitting trot. The power fluctuations in the spring of the rider are much larger than those during sitting trot, a consequence of the much lower spring stiffness of the rider in combination with the counter-movement between rider and horse, which results in much larger length changes in the rider's spring. The net energy that is transmitted from the horse to the rider is extremely small for the simulated jockey stride (6.7 J per stride cycle). The forcing function of the horse produces much higher positive power peaks (about 6000 W) with the simulated jockey technique than for sitting trot; larger power peaks occur for the horse's spring, and more power is lost to damping (Fig. 6R), which is in agreement with the large vertical excursion of the horse. Over the stride, the net power of the forcing function is almost exclusively spent on damping losses of the horse. The free-fall phases of the horse are longer with the jockey technique than for sitting trot.

Rising trot cannot be simulated adequately based on optimization of the (constant) spring stiffness and damping coefficient of the rider. With the time-dependent forcing function incorporated into the model, it is possible to simulate rising trot (Fig. 6C,G,K,O,S),

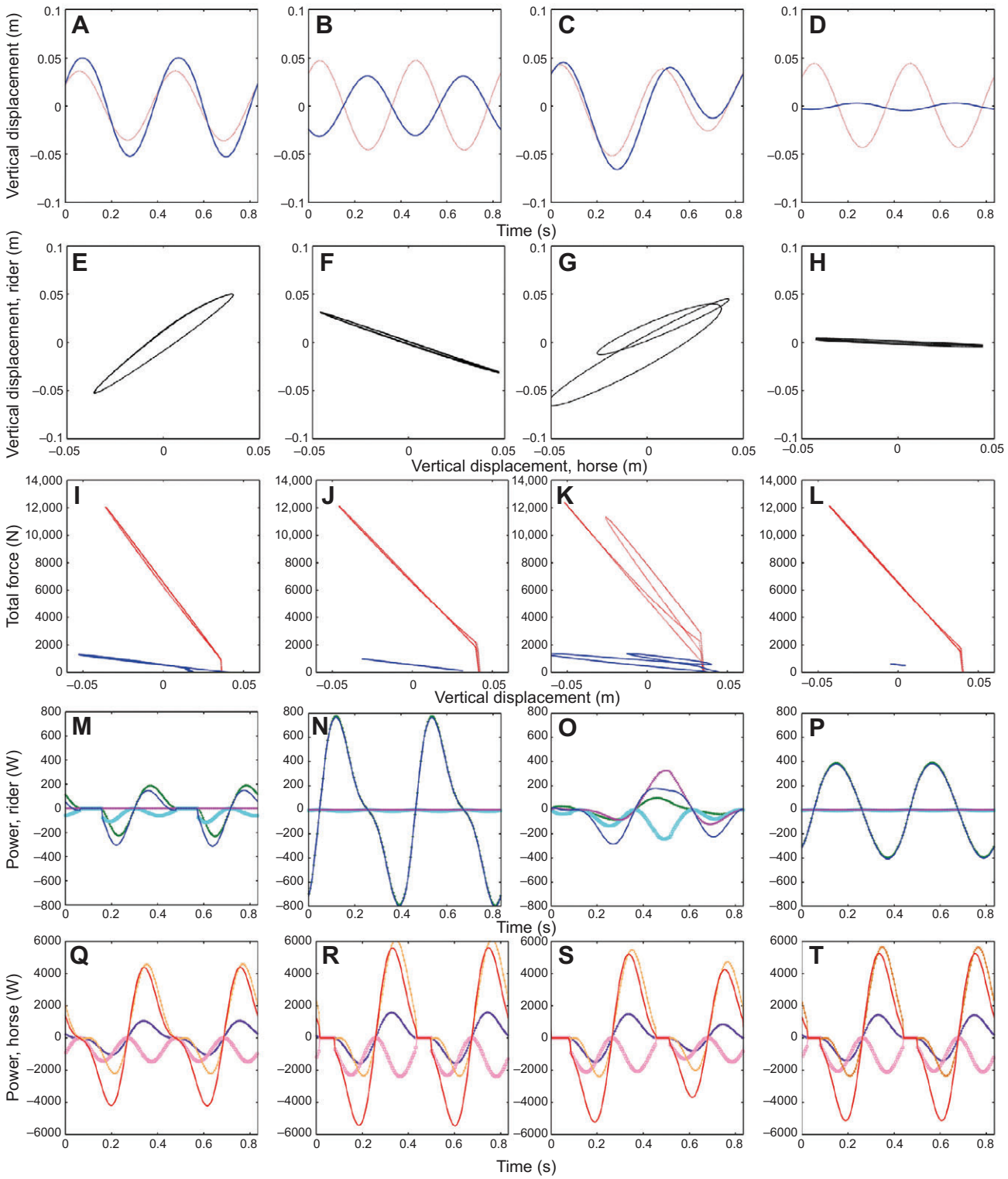

Fig. 6. Result of optimization based on vertical displacement and minimal peak rider force and minimal work of the horse in simulation model 2. (A) Vertical displacement during sitting trot. (B) Vertical displacement during modern jockey technique. (C) Vertical displacement during rising trot with forcing function. (D) Vertical displacement during optimal horse-riding technique (extreme jockey technique). (E) Phase plot of sitting trot. (F) Phase plot of modern jockey technique. (G) Phase plot of rising trot with forcing function. (H) Phase plot of optimal horse-riding technique. (I) Work loops of horse and rider at sitting trot. (J) Work loops of horse and rider with modern jockey technique. (K) Work loops of horse and rider at rising trot with forcing function. (L) Work loops of horse and rider with optimal horse-riding technique. (M) Power of rider at sitting trot. (N) Power of rider with modern jockey technique. (O) Power of rider at rising trot with forcing function. (P) Power of rider with optimal horse-riding technique. (Q) Power of horse at sitting trot. (R) Power of horse with modern jockey technique. (S) Power of horse at rising trot with forcing function. (T) Power of horse with optimal horse-riding technique. Red dotted line, vertical displacement, work loops, horse; blue solid line, vertical displacement, work loops, rider. Power in M–P: blue solid line, total of spring, damping and forcing function; green crosses, spring; light blue squares, damping; purple crosses, forcing function. Power in Q–T: red solid line, total of spring, damping and forcing function; purple crosses, spring; pink squares, damping; yellow crosses, forcing function.

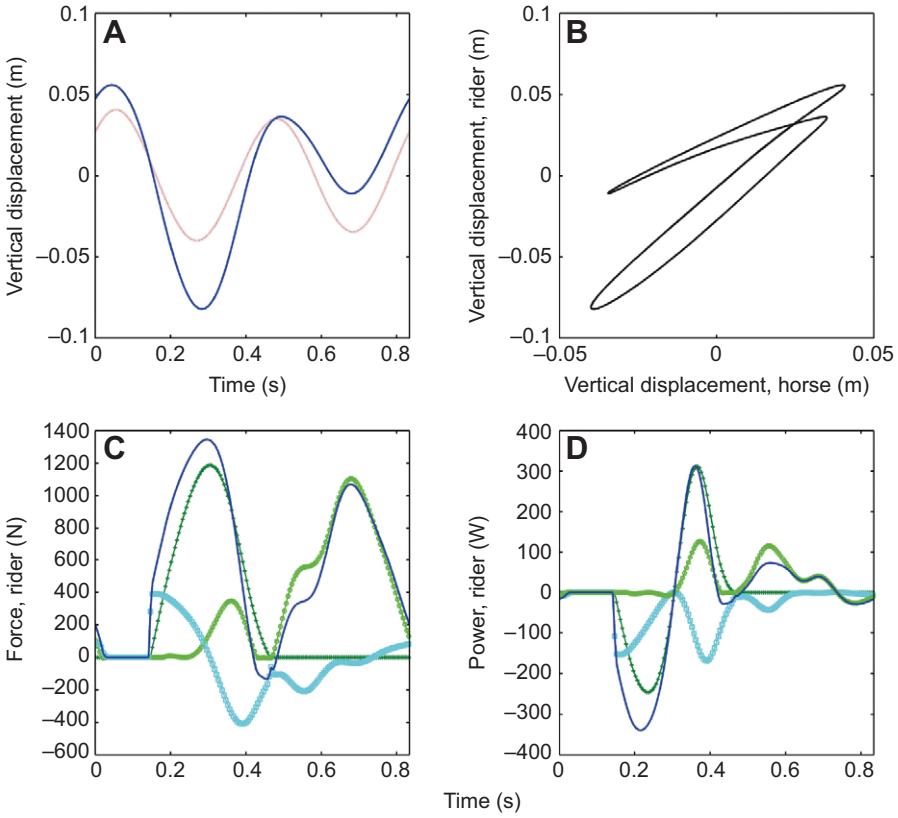

Fig. 7. Simulation of rising trot with active spring system for the leg of the rider with model 3. (A) Vertical displacement. (B) Phase plot. (C) Force of the rider. (D) Power of the rider. Red dotted line, vertical displacement and power of horse; blue solid line, vertical displacement and power of rider. Force and power in C,D: blue solid line, total of saddle spring, leg spring and damping; green crosses, saddle spring; light green circles, leg spring; light blue squares, damping.

although the agreement with the experimental data is not optimal. The spring stiffness and damping coefficient needed to simulate rising trot as closely as possible are relatively low (4.8 kN m^{-1}) and high (2779 kg s^{-1}), respectively. The power of the forcing function of the rider fluctuates more strongly than those of the simulated sitting trot and jockey technique, and the power of the rider's damper shows a stronger negative peak. This indicates that the rider has to spend more energy during rising trot than during sitting trot or jockey riding. The power fluctuations of the horse resemble those of sitting trot during half of the stride and jockey riding during the other half, albeit the peak power of the forcing function is somewhat reduced. The total work of the horse is 31 J per stride cycle in this simulated rising trot.

The lowest work of the horse (4.2 J per stride cycle) and lowest peak force of the rider (1.04; dimensionless: peak force/body weight of rider) are both a result of a relatively low spring stiffness (0.6 kN m^{-1}) and low damping of the rider (19 kg s^{-1}). The result is an 'extreme' jockey technique simulated in Fig. 6D,H,L,P,T, associated with a very limited motion of the rider. With the same forcing function of the horse, the motion of the horse is reduced compared with that for the jockey technique performed in daily practice (Fig. 6B) because of the reduced counter-motion of the rider, which tends to lead to greater fluctuation of the combined centre of mass of horse and rider. The power fluctuations of the rider's spring are now much lower than for the normal jockey technique (Fig. 6P and 6N). The power of the horse lost in damping is slightly lower for the extreme jockey technique than for the normal jockey technique. Thus, overall energy expenditure is also slightly lower.

Finally, the third spring–damper–mass model, with a more elaborate spring system of the rider, enabled the simulation of all three riding styles with a good correspondence with the experimental data. Here, we will restrict the results to the simulation of rising trot, which has a far better agreement with the experimental data (Fig. 7) than could be achieved with model 2. The parameters of the model were optimized to simulate a rising trot as shown in Fig. 2. Fig. 7A shows the simulated displacements of rider and horse, which resembles the typical pattern for the rider also shown in Fig. 2B. Fig. 7B shows the phase plot of rider displacement against horse displacement, which is now closer to the experimental loop of Fig. 2D. The leg spring shows a small force peak of 347 N (Fig. 7C), just before the lift off from the saddle, and a second large peak of 1104 N during the rising phase (second part of the stride). The force of the saddle spring is single peaked during the sitting phase. Both springs have a zero force during a short free-fall phase. The damping force shows both positive and negative force peaks. The power of the saddle spring fluctuates from negative to positive while the rider is seated (Fig. 7D). The net work over the stride is zero for this spring. The active leg spring has two positive peaks in excess of 100 W and a few minor negative peaks. Overall the leg spring produces 20 J per stride cycle of positive work, which is possible because of the varying stiffness and resting length throughout the stride, which gives the 'spring' muscle-like properties. Much of this work is used to compensate for the power losses in the rider's damping.

DISCUSSION

In the search for general principles underlying bouncing gaits, biomechanics have modelled the human body as a linear mass-less spring supporting a point mass equivalent to the body mass. The term 'leg spring' is typically used to indicate stiffness of the spring, which is determined by the relationship between ground reaction force and distance between the centre of mass and the centre of pressure on the ground (Bobbert and Casius, 2011). The leg spring therefore not only refers to the biomechanical properties of the leg but also represents the whole body. The stiffness of the leg spring has been determined in a variety of bouncing gaits of humans. During running, the stiffness of the leg spring is relatively constant,

ranging between 11 and 19 kN m^{-1} (Blum et al., 2009). When humans hop in one place they can vary the stiffness of their leg spring by changing the hopping height or frequency. Stiffness values between 9 and 45 kN m^{-1} have been found (Bobbert and Casius, 2011; Farley et al., 1991). To our knowledge, the stiffness of the leg spring has not been determined for the different riding techniques that a rider can use in equestrian sports.

In this research, three spring (–damper)–mass models were developed to provide insight into the mechanisms of these horse-riding techniques. The first approach involved constructing a simple spring–mass model in which the musculoskeletal systems of both the horse and rider are considered mechanically as linear spring–mass systems. The spring–mass system of the horse is actively driven. Each system is assumed to behave like a point mass bouncing on a mass-less spring without viscous losses, which is the simplest model possible for any bouncing system.

Although such a simple model may provide useful information on the strategies a rider can use to respond to the movement of the horse, it has limitations. In the simple spring–mass model the horse maintains contact with the ground during locomotion; this is not true for trotting, which has two phases in each stride when the feet lose contact with the ground (the suspension phases). Although the rider maintains contact with the horse, the rider and the horse are not attached to each other. The looseness of this contact can be modelled by combining the spring–mass model with a free-fall of horse and rider. Furthermore, as the legs of both horse and rider have damper-like functions and as there is a phase shift between the motions of horse and rider (Lagarde et al., 2005), dampers for both horse and rider were implemented in the model. During rising trot, the rider actively stands up and two approaches were used to simulate the rider's muscle activation. The second spring–damper–mass model incorporates a free-fall, dampers for both horse and rider and a forcing function for the rider. The third spring–damper–mass model incorporates a free-fall, dampers for both horse and rider and an active spring system for the legs of the rider with varying stiffness and rest length.

In sitting trot, the rider stays seated in the saddle. The movement of the rider is influenced by the saddle, and by the skin, the back and abdominal muscles and the lower back flexion of the rider. The influence of the rider's legs is probably limited during sitting trot because the forces on the stirrups are low (van Beek et al., 2011). Therefore, it is likely that the rider's lower back is the dominant factor for the mechanical properties of the rider during sitting trot. The required effective stiffness of the leg spring of the rider is indeed high for sitting trot compared with other human athletic activities, such as running. In this range of high spring stiffness of the rider, the vertical displacement and force of the rider are not very sensitive to a change in spring stiffness (Fig. 4B,D). Note that the spring stiffness was kept constant during the stride in these simulations with the simple model.

When the rider stands in the stirrups in the jockey position, their legs determine the mechanical properties of the rider. The required stiffness of the leg spring of the rider for the modern jockey technique is low compared with other human athletic activities. In this range of low spring stiffness of the rider, vertical displacement of the rider is very sensitive to a change in spring stiffness (Fig. 4B). This could mean that control of leg stiffness in this position is crucial. Between these two ranges of spring stiffness there is a resonance zone with very high and unrealistic displacements and forces (Fig. 4C,D).

In the extended spring–damper–mass models, the horse is no longer fixed to the ground and the rider is no longer fixed to the horse. This extension to the model was made because at trot there are two phases in each stride when none of the feet are in contact with the ground (the suspension phases) and although the rider maintains contact with the horse, the rider and the horse are not attached to each other. The looseness of this attachment was modelled by combining the spring–damper–mass models with a free-fall. It is striking that for the two riding modes, sitting trot and modern jockey technique, it is possible to have a stable cyclic simulation with a suspension phase of the rider. This raises the question of whether the rider does in fact have a suspension phase. In fact, both the total vertical force on the rider and the stirrup force do reach zero during sitting trot (de Cocq et al., 2010; van Beek et al., 2011). This supports the idea that there is a suspension phase at sitting trot, although this might not be visible to the eye.

A wide range of combinations of the rider's spring stiffness and damping coefficients result in a sitting trot. An increase in damping coefficient will increase the work required of the horse and an increase of spring stiffness will increase the peak forces on the rider and therefore on the horse's back. This indicates that there is an optimal combination of damping coefficient and spring stiffness of the rider. The modern jockey technique has high peaks in the power of the rider and is therefore the most demanding technique for the rider.

In the simulation of rising trot using the extended spring–damper–mass model with an active spring system for the leg of the rider, the force patterns of the total force on the saddle resemble the forces measured previously (de Cocq et al., 2010). The spring leg forces resemble the stirrup forces measured by van Beek and colleagues (van Beek et al., 2011), which have a small force peak in the sitting phase and a large force peak in the standing phase. However, the timing of the first small peak of the spring leg force is relatively early compared with that of the measured stirrup forces. In the model, the timing of the change in spring stiffness and rest length of the active spring system of the leg was kept the same. In real life, there is probably a timing difference between the change in spring stiffness and rest length. This could explain the observed difference between the simulated spring leg force and measured stirrup forces. During the sitting phase, the forces on the rider are indeed dominated by the saddle spring. During the standing phase, the saddle spring loses contact with the horse and the active spring system of the leg of the rider takes over.

The lowest work of the horse and lowest peak force of the rider are both a result of relatively low spring stiffness and low damping of the rider. This combination has an even greater effect than the modern jockey technique. When the goal is to reduce peak forces on the horse's back and to reduce the energy expenditure of the horse, this mode seems to be the preferred mode for horse–rider interaction.

A topic for further research is how the rider actually changes their biomechanical properties. These biomechanical properties result from the complex interplay between muscle stimulation time histories, muscle properties and geometry. Research on riding techniques, measuring kinematics, forces between horse and rider and electromyography of the leg muscles of the rider, is needed to tackle this problem.

CONCLUSIONS

The models developed here provide insight into the biomechanical requirements a rider has to comply with in different riding techniques. At sitting trot, the rider is able to follow the movement of the horse by using a relatively high spring stiffness and a high damping coefficient. The modern jockey technique results from of

a relatively low spring stiffness and a low damping coefficient. Rising trot requires an active spring system for the leg of the rider, which changes in both stiffness and rest length. An 'extreme' modern jockey technique is the optimal mode for the minimization of both vertical peak force of the rider and mechanical work of the horse. The models confirm the hypothesis that the connection between horse and rider has a relatively low spring stiffness in the riding technique with least loading and that this riding technique is an example of a strategy that reduces the peak forces on and the energy expenditure of the carrier.

LIST OF SYMBOLS AND ABBREVIATIONS

c	damping coefficient
f	frequency of a bounce
F_0	amplitude of the forcing function
g	magnitude of the gravitational acceleration
h	horse (subscript)
k	spring stiffness
l	active spring system of the leg of the rider (subscript)
m	mass
r	rider (subscript)
s	saddle spring of the rider (subscript)
t	time
z, $\dot{z}$, $\ddot{z}$	vertical displacement, velocity and acceleration
γ	phase difference of the forcing function
δ_{st}	static deflection due to the weight of the mass acting on the spring
ε	strain
η	force contact factor
ω	angular frequency of the forcing function

ACKNOWLEDGEMENTS

We thank the riders who participated in the experiment. Special thanks are due to LeeAnn Kaiser for her invaluable technical support and Maarten Bobbert for his insightful comments on an early version of the manuscript.

AUTHOR CONTRIBUTIONS

All authors were involved in the conception, design and execution of the study, the interpretation of the findings, and the drafting and revising of the article. P.d.C. and H.M.C. executed the experimental work, P.d.C. and M.M. constructed the simple model and P.d.C. and J.L.v.L constructed the extended models.

COMPETING INTERESTS

No competing interests declared.

FUNDING

This research received no specific grant from any funding agency in the public, commercial, or not-for-profit sectors.

REFERENCES

Abe, D., Yanagawa, K. and Niihata, S. (2004). Effects of load carriage, load position, and walking speed on energy cost of walking. *Appl. Ergon.* **35**, 329-335.
Abe, D., Muraki, S. and Yasukouchi, A. (2008). Ergonomic effects of load carriage on the upper and lower back on metabolic energy cost of walking. *Appl. Ergon.* **39**, 392-398.
Bastien, G. J., Schepens, B., Willems, P. A. and Heglund, N. C. (2005). Energetics of load carrying in Nepalese porters. *Science* **308**, 1755.
Blum, Y., Lipfert, S. W. and Seyfarth, A. (2009). Effective leg stiffness in running. *J. Biomech.* **42**, 2400-2405.
Bobbert, M. F. and Richard Casius, L. J. (2011). Spring-like leg behaviour, musculoskeletal mechanics and control in maximum and submaximum height human hopping. *Philos. Trans. R. Soc. B* **366**, 1516-1529.
de Cocq, P., Prinsen, H., Springer, N. C. N., van Weeren, P. R., Schreuder, M., Muller, M. and van Leeuwen, J. L. (2009). The effect of rising and sitting trot on back movements and head-neck position of the horse. *Equine Vet. J.* **41**, 423-427.
de Cocq, P., Duncker, A. M., Clayton, H. M., Bobbert, M. F., Muller, M. and van Leeuwen, J. L. (2010). Vertical forces on the horse's back in sitting and rising trot. *J. Biomech.* **43**, 627-631.
Farley, C. T., Blickhan, R. and Taylor, C. R. (1985). Mechanics of human hopping: model and experiments. *Am. Zool.* **25**, 54A.
Farley, C. T., Blickhan, R., Saito, J. and Taylor, C. R. (1991). Hopping frequency in humans: a test of how springs set stride frequency in bouncing gaits. *J. Appl. Physiol.* **71**, 2127-2132.
Farley, C. T., Glasheen, J. and McMahon, T. A. (1993). Running springs: speed and animal size. *J. Exp. Biol.* **185**, 71-86.
Foissac, M., Millet, G. Y., Geyssant, A., Freychat, P. and Belli, A. (2009). Characterization of the mechanical properties of backpacks and their influence on the energetics of walking. *J. Biomech.* **42**, 125-130.
Heglund, N. C., Willems, P. A., Penta, M. and Cavagna, G. A. (1995). Energy-saving gait mechanics with head-supported loads. *Nature* **375**, 52-54.
Kram, R. (1991). Carrying loads with springy poles. *J. Appl. Physiol.* **71**, 1119-1122.
Lagarde, J., Kelso, J. A. S., Peham, C. and Licka, T. (2005). Coordination dynamics of the horse-rider system. *J. Mot. Behav.* **37**, 418-424.
Marsh, R. L., Ellerby, D. J., Henry, H. T. and Rubenson, J. (2006). The energetic costs of trunk and distal-limb loading during walking and running in guinea fowl *Numida meleagris*: I. Organismal metabolism and biomechanics. *J. Exp. Biol.* **209**, 2050-2063.
McGuigan, M. P. and Wilson, A. M. (2003). The effect of gait and digital flexor muscle activation on limb compliance in the forelimb of the horse *Equus caballus*. *J. Exp. Biol.* **206**, 1325-1336.
Nelder, J. A. and Mead, R. (1965). A simplex-method for function minimization. *Comput. J.* **7**, 308-313.
Pearson, R. A., Dijkman, J. T., Krecek, R. C. and Wright, P. (1998). Effect of density and weight of load on the energy cost of carrying loads by donkeys and ponies. *Trop. Anim. Health Prod.* **30**, 67-78.
Peham, C., Scheidl, M. and Licka, T. (1999). Limb locomotion – speed distribution analysis as a new method for stance phase detection. *J. Biomech.* **32**, 1119-1124.
Peham, C., Licka, T., Kapaun, M. and Scheidl, M. (2001). A new method to quantify harmony of the horse–rider system in dressage. *Sports Eng.* **4**, 95-101.
Peham, C., Kotschwar, A. B., Borkenhagen, B., Kuhnke, S., Molsner, J. and Baltacis, A. (2010). A comparison of forces acting on the horse's back and the stability of the rider's seat in different positions at the trot. *Vet. J.* **184**, 56-59.
Pfau, T., Spence, A., Starke, S., Ferrari, M. and Wilson, A. (2009). Modern riding style improves horse racing times. *Science* **325**, 289.
Roepstorff, L., Egenvall, A., Rhodin, M., Byström, A., Johnston, C., van Weeren, P. R. and Weishaupt, M. (2009). Kinetics and kinematics of the horse comparing left and right rising trot. *Equine Vet. J.* **41**, 292-296.
Rome, L. C., Flynn, L., Goldman, E. M. and Yoo, T. D. (2005). Generating electricity while walking with loads. *Science* **309**, 1725-1728.
Rooney, J. R. (1986). A model for horse movement. *J. Equine Vet. Sci.* **6**, 30-34.
Schöllhorn, W. I., Peham, C., Licka, T. and Scheidl, M. (2006). A pattern recognition approach for the quantification of horse and rider interactions. *Equine Vet. J.* **Suppl. 36**, 400-405.
Slijper, E. J. (1946). Comparative biologic-anatomical investigations on the vertebral column and spinal musculature of mammals. *Proc. K. Ned. Acad. Wetensch.* **42**, 1-128.
Taylor, C. R., Heglund, N. C., McMahon, T. A. and Looney, T. R. (1980). Energetic cost of generating muscular force during running – a comparison of large and small animals. *J. Exp. Biol.* **86**, 9-18.
van Beek, F. E., de Cocq, P., Timmerman, M. and Muller, M. (2011). Stirrup forces during horse riding: a comparison between sitting and rising trot. *Vet. J.* **193**, 193-198.
Zadpoor, A. A. and Nikooyan, A. A. (2010). Modeling muscle activity to study the effects of footwear on the impact forces and vibrations of the human body during running. *J. Biomech.* **43**, 186-193.
Zatsiorsky, V. M. (2002). *Kinetics of Human Motion*, 590 pp. Champaign, IL: Human Kinetics Publishers.